Probing essential nucleobase functional groups in aptamers and deoxyribozymes by nucleotide analog interference mapping of DNA

Falk Wachowius and Claudia Höbartner*

Research Group Nucleic Acid Chemistry, Max Planck Institute for Biophysical Chemistry, Göttingen, Germany

Table of Contents

Materials

Standard 5'-*O*-DMT-protected 3'-β-cyanoethyl phosphoramidites of N^6-benzoyl-2'-deoxyadenosine, N^4-benzoyl-2'-deoxycytidine, N^2-(*N*,*N*-dimethylamino)methylene-2'-deoxyguanosine, and thymidine were from SAFC/Sigma-Aldrich. Benzylthiotetrazole (BTT) was from Carbosynth (UK). Ribonucleotide triphosphates (NTPs) for in vitro transcription reactions were purchased from Jena Bioscience. α-^{32}P-dATP (3000 Ci/mmol) and γ-^{32}P-ATP (3000 Ci/mmol) were from Perkin Elmer. T4 RNA ligase and T4 polynucleotide kinase (PNK) were from Fermentas, and Klenow fragment, 3'→5' exo$^-$, DNA polymerase I was from Jena Bioscience. ATP-agarose (9 atom linker to C8, CNBr-activated, cross-linked 4% beaded agarose) was from Sigma Aldrich.

The structures of ribonucleoside phosphoramidites used in this study are depicted in Figure S1. 2'-*O*-TOM-protected 3'-β-cyanoethyl phosphoramidites of N^6-acetyladenosine (A), N^4-acetylcytidine (C), N^2-acetylguanosine (G), and uridine (U), as well as 2'-*O*-TBDMS protected phosphoramidites of Purine (P), Inosine (I), N^6-benzoyl-7-deazaadenosine (c^7A), N^2-isobutyl-7-deazaguanosine (c^7G), N^4-benzoyl-5-methylcytosine (m^5C) were purchased from ChemGenes, USA. 2'-*O*-TBDMS-protected Zebularine (Z) was obtained from Berry Associates, USA. 2'-*O*-TOM protected m^3U phosphoramidite (m^3U) was a gift from Prof. Ronald Micura, University of Innsbruck. 2'-*O*-TOM protected phosphoramidites of methylated ribonucleosides N^6,N^6-dimethyladenosine ($m^6{}_2$A), N^2-acetyl-1-methylguanosine (m^1G), O^6-(4-nitrophenyl)-N^2-methylguanosine (m^2G) and O^6-(4-nitrophenyl)-N^2,N^2-dimethylguanosine ($m^2{}_2$G) were synthesized according to published procedures.[1] 2'-*O*-TOM protected N^2-acetyl-2-aminopurine (AP) phosphoramidite was also synthesized as described.[2] (This compound was earlier commercially available from GlenResearch, USA, but has been discontinued. Alternatively, 2'-*O*-TBDMS-protected N^2-isobutyryl-2-aminopurine phosphoramidite is now available from GlenResearch and ChemGenes).

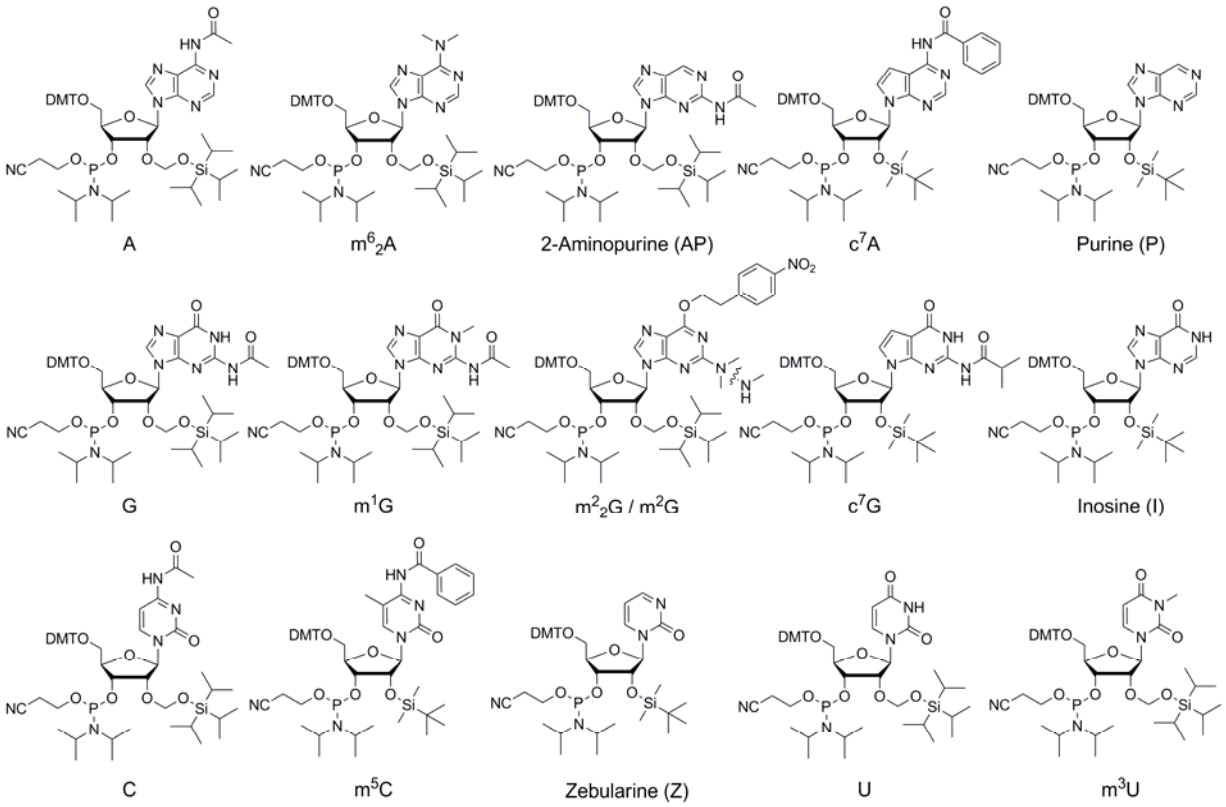

Figure S1. Ribonucleotide phosphoramidites used in this study.

Oligonucleotides

AMP-DNA aptamer

5′-ACCTGGGGGAGTATTGCGGAGGAAGGT-3′

RNA substrates for deoxyribozymes

7S11 L-RNA 5′-GGAAUACGACUCAC-3′
7S11 R-RNA 5′-pppGGAAGAGAUGG-3′
9DB1L-RNA 5′-GGAAGUCUCAUGUACUA-3′
9DB1R-RNA 5′-pppGAUGUUCUAGCGCCGGA-3′

The RNA substrates for deoxyribozymes were prepared by in vitro transcription using T7 RNA polymerase and a synthetic DNA template.[3-4]

Deoxyribozyme sequence

7S11 5′-CAACATCTC**CAGTGCAGGGC**GTGAG**GGCTCGG***TTCC***CGTATTCC-3′
9DB1* 5′-CAAGGCGCTAGAACAT**GGATCATACGGTCGGAGGGGTTTGCCGTTTA**AGTACATGAGACTTCC-3′

The bold nucleotides represent the catalytic loop regions, and the non-bold nucleotides constitute the binding regions for the RNA substrates. The bold underlined nucleotides form a Watson-Crick base-paired stem. Modified nucleotide analogs were statistically incorporated only into the bold region.

Template DNA oligonucleotides for 3'-^{32}P-labeling

for 7S11 5′-GTGGAATACGGGAA-3′
for 9DB1 5′-GTGGAAGTCTCATGTACT-3′

Solid-phase synthesis, deprotection and purification

Solid-phase synthesis was performed on 0.7 µmol polystyrene custom primer supports from GE Healthcare, using a Pharmacia Gene Assembler Plus. Phosphoramidite solutions, tetrazole solution, and acetonitrile were dried over activated molecular sieves overnight. All sequences were prepared DMT-off.
Synthesis conditions were as follows:
Detritylation: 3% (v/v) dichloroacetic acid in 1,2-dichloroethane for two minutes.
Activation and coupling: 75 µl of 0.1 M phosphoramidites in acetonitrile (see below for details on phosphoramidite mixtures for library syntheses); 250 µl of 0.25 M benzyl thiotetrazole in acetonitrile;
Coupling time: 2 min (for all DNA coupling steps and for 2'-TOM-rM/dN mixtures) or 4 min (for 2'-TBDMS-rM/dN mixtures).
Capping: 1:1 (v/v) A/B for one minute (A, Ac_2O/sym-collidine/acetonitrile, 2:3:5 (v/v); B, 0.5 M 4-(dimethylamino)pyridine in acetonitrile).
Oxidation: 10 mM I_2 in acetonitrile/sym-collidine/water (10:1:5, v/v) for one minute.

Deprotection of ribonucleotide-containing deoxyribozyme libraries was achieved with 25% ammonium hydroxide:ethanol 3:1 for 16 hours at 55°C, followed by cleavage of the 2'-*O*-silyl groups with tetrabutylammonium fluoride trihydrate (TBAF·$3H_2O$) in THF (1 M, 500 µL) at 37°C for 5 hours. The reaction was quenched with Tris.HCl (1 M, pH 7.4, 500 µL), and the crude oligonucleotides were isolated by desalting on a Sephadex G 10 column (3x5 ml HiTrap column, GE Healthcare) monitored by UV-detection at 280 nm.

The quality of the synthesized oligonucleotide libraries was analyzed by anion exchange HPLC (Dionex DNAPac PA200 column: eluant A, 25 mM Tris.HCl, pH 8.0, 6 M urea; eluant B, 25 mM Tris.HCl, pH 8.0, 0.5 M $NaClO_4$, 6 M urea) and then purified by denaturing PAGE [12% polyacrylamide, 1x TBE (89 mM each Tris and boric acid, pH 8.3, 2 mM EDTA), 7 M urea, 0.7 mm, 20x30 cm, 35W]. Oligonucleotides were visualized by UV shadowing and extracted by crush and soak into TEN (10 mM

Tris.HCl, pH 8.0, 1 mM EDTA, 300 mM NaCl) at 37°C for 2x 3-5h, followed by precipitation with ethanol at –80°C. The quality was confirmed by denaturing anion-exchange HPLC as above.

Coupling efficiency of modified RNA phosphoramidites in presence of DNA phosphoramidites

The incorporation efficiency of 2'-TOM-protected ribonucleotide phosphoramidites in competiton with deoxribonucleotide phosphoramidites has been determined previously.[4] Here we checked the incorporation efficiency of each nucleobase-modified RNA phosphoramidite in the mixture with the parent deoxyribonucleotide phosphoramidite by synthesizing 5-mer model oligonucleotides of the sequence ACGTT, in which one coupling step was performed with rM/dN = 15/85 mixtures (i.e., mixtures of 15% ribonucleoside analog and 85% deoxyribonucleoside of the parent unmodified nucleobase). The mixtures of unmodified DNA pentamer and oligonucleotides containing one 2'-*O*-TOM (or 2'-*O*-TBDMS)-protected ribonucleotide were analyzed by denaturing anion exchange HPLC. The ratio of unmodified and 2'-*O*-TOM/TBDMS-rM-containing pentamer was determined by integration of the area under the peaks (detected at 260 nm). The experimentally determined value for ribonucleotide incorporation was 4-10% (generally, 2'-TOM-protected phosphoramidites were incorporated at somewhat higher ratios than 2'-TBDMS protected phosphoramidites, despite the longer coupling time used for TBDMS-containing mixtures. The lowest incorporation ratios were observed for cytidine and its analogs). The optimal incorporation rates were calculated using the approach described for CoMA.[4] For example for the 9DB1* core, the desired incorporation rates are 6% for guanosines (12 positions), 8% for thymidines (9 positions), and 10% for adenosines and cytidines (5 positions), in order to obtain at least 30% of monosubstituted DNA but keep the probability for multiply substituted derivatives below 15%.

Nucleotide analog interference mapping of DNA

dNAIM of ATP/AMP aptamer

The aptamer libraries were 5'-^{32}P-labeled using γ-^{32}P-ATP and PNK. The active (AMP binding) fraction was separated by affinity chromatography on ATP-agarose (1.9 μmol ATP/mL packed gel, column volume 40 μL in a spin column device, placed inside a standard 1.5 mL sample tube). The column was washed with 12 column volumes (CV) of column buffer (300 mM NaCl, 5 mM $MgCl_2$, in 20 mM Tris.HCl, pH 7.6). The DNA was applied in 2 CV of column buffer and the mixture was incubated for 5 min. The unbound fraction was collected by centrifugation (3000 rpm, 30 sec) and saved for analysis. The column was washed with 10 CV of column buffer, and the bound DNA aptamers were then eluted with 1 CV of 3 mM ATP in column buffer. The DNA of the unbound (inactive flow-through) and the active (eluted with ATP) fractions was isolated by ethanol precipitation, and then subjected to alkaline hydrolysis using 100 mM NaOH at 95°C for 10 min. The hydrolysis products were resolved on denaturing sequencing gels (15% acrylamide, 7M urea, 1xTBE, 0.4 mm, 20x30cm, 35W, 1h). Gels were dried at 80°C under vacuum for 30 min, and exposed to a Phosphor storage screen. The full gel image for the unselected library, the active and the inactive fractions is depicted in Figures S2.

dNAIM of RNA-ligating deoxyribozymes

The deoxyribozyme libraries were 5'-phosphorylated using ATP and PNK, then ligated to the R-RNA substrate using T4 RNA ligase, and 3'-^{32}P-labeled using templated dATP addition with Klenow fragment. All steps were performed using similar conditions as reported for CoMA.[4] The 9DB1 DNA-catalyzed ligation reaction was performed at pH 9.0 in the presence of 40 mM $MgCl_2$. The reactions were run for 3 hours at 37°C. The ligation yields for all synthesized libraries are summarized in Tables S1 and S2. The ligation products were isolated by PAGE and then subjected to alkaline hydrolysis using 100 mM NaOH at 95°C for 10 min. The hydrolysis products were resolved on denaturing sequencing gels (20% acrylamide, 7M urea, 1xTBE, 0.4 mm, 20x40cm, 35W). Gels were dried at 80°C under vacuum for 30 min, and exposed to a Phosphor storage screen. The full gel images for the 8 synthesized 7S11 dNAIM libraries are depicted in Figure S4, and for all 17 synthesized 9DB1 dNAIM libraries in Figures S6 – S7.

Analysis and quantification of interference pattern

The analysis of dNAIM gels followed similar procedures as described for the analysis of NAIM data for RNA[5-6] and CoMA for DNA.[4] Individual band intensities were quantified using ImageQuant software (Molecular Dynamics). Volume and area analysis tools were both used and gave similar results. As an example, line graphs of the hydrolysis pattern of the c^7G library fractions used for area analysis are shown in Figure S8. The overall area under the curve was normalized for minor loading differences, and the interference values were calculated for every nucleotide position as the ratio of corresponding peak areas in both graphs. For some dNAIM libraries, the hydrolysis efficiency was rather low, and the un-cleaved band was saturated. In these instances, calculation of the interference effect was performed as described for CoMA.[4] Values <2 (i.e., less than 50% change in intensity) were considered insignificant and colored green, values from 2 to 6 were termed small or moderate interference values and colored orange, and interference values >6 were termed strong and colored red. Interference values that were larger than ten were cut off at 10.0. Interference values were obtained from three to four individual hydrolysis experiments, using two to three independent library separations. The hydrolysis pattern and interference values were well reproducible, and the experimental error was below 15%. The interference values for individual rM-containing aptamer libraries are depicted in Figure S2, for 7S11 deoxyribozyme libraries in Figure S5, and for 9DB1* libraries in Figure S10. A schematic representation of the interference effects on the secondary structure of the 9DB1* core is given in Figure S9.

a) b)

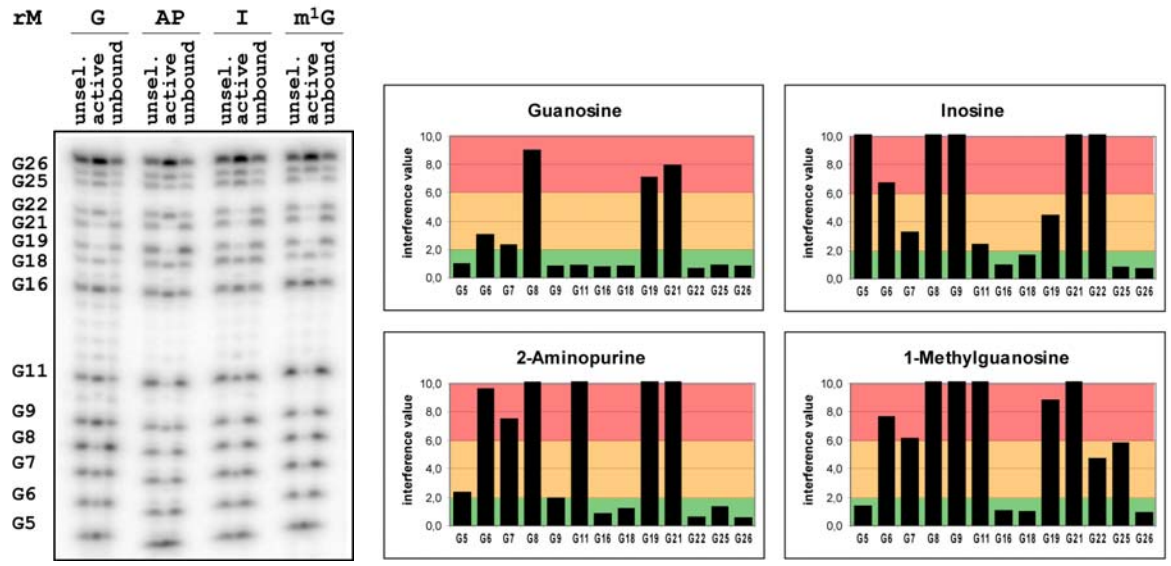

Figure S2. a) Full alkaline hydrolysis gel of AMP aptamer showing unselected library, active and unbound fractions. b) Quantitative interference values calculated from the ratio of band intensities in the active fraction and the unselected library (average of three individual analyses, normalized for position G16; the variability between individual experiments was less than 20% (slightly higher for the aptamer than for the deoxyribozymes)).

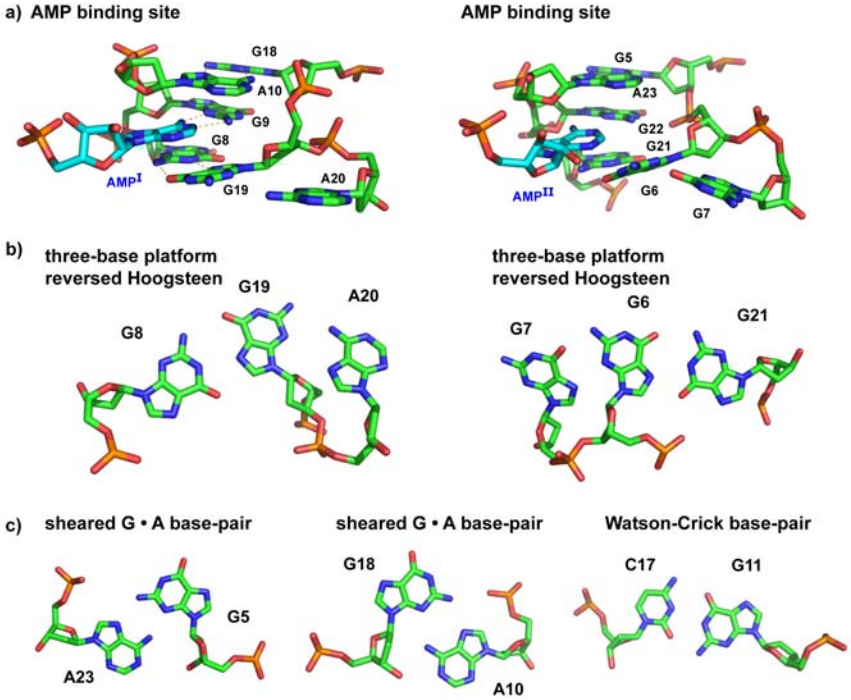

Figure S3. Molecular interactions in the AMP aptamer. a) The AMP ligands are recognized via H-bonding of their Watson-Crick edge to the minor groove edge of guanosines. AMP-I pairs with G9, and AMP-II with G22. b) The crucial three-base-platforms (G8•G19)•A20 and G7• (G6•G21) contain reverse Hoogsteen base-pairs. The strongest OH effects in the dNAIM data for G8, G19 and G21 can be rationalized based on the involvement in these three-base-platforms. c) The sheared G•A base-pairs involving G5 and G18 form the outermost mismatches of the aptamer core, and are less sensitive to substitution by nucleotide analogs AP, I and m^1G. The strong interference effects for AP and m^1G at position 11 are consistent with the formation of a critical Watson-Crick base-pair. Similary, the Watson-Crick base-pair C3-G25 does not tolerate m^1G subsitution.

Table S1. Yield of DNA-catalyzed RNA ligation by 7S11 dNAIM libraries

DNA library	rG	m^1G	$m^2{}_2G$	m^2G	AP	I	P	c^7G
ligation yield (%) after 3h	53	45	54	40	48	45	44	48

Table S2. Yield of DNA-catalyzed RNA ligation by 9DB1* dNAIM libraries

DNA library	rG	m^1G	$m^2{}_2G$	AP	I	P(G)	c^7G
ligation yield (%) after 3h[a]	24	17	28	17	29	28	23

	rA	c^7A	$m^6{}_2A$	P(A)	rC	Z(C)	m^5C
ligation yield (%) after 3h[a]	22	19	17	21	24	23	25

	rU	Z(T)	m^3U
ligation yield (%) after 3h[a]	17	15	12

[a] mean of 2-3 independent experiments, max 5-10% deviation between individual experiments

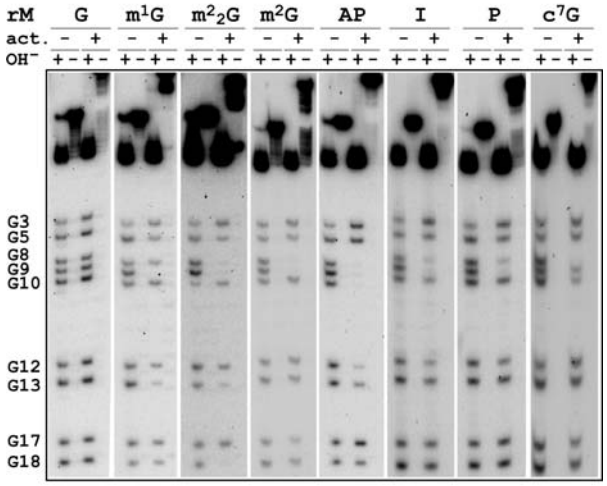

Figure S4. Full images of alkaline hydrolysis gels of 7S11 dNAIM libraries with guanosine nucleotide analogs.

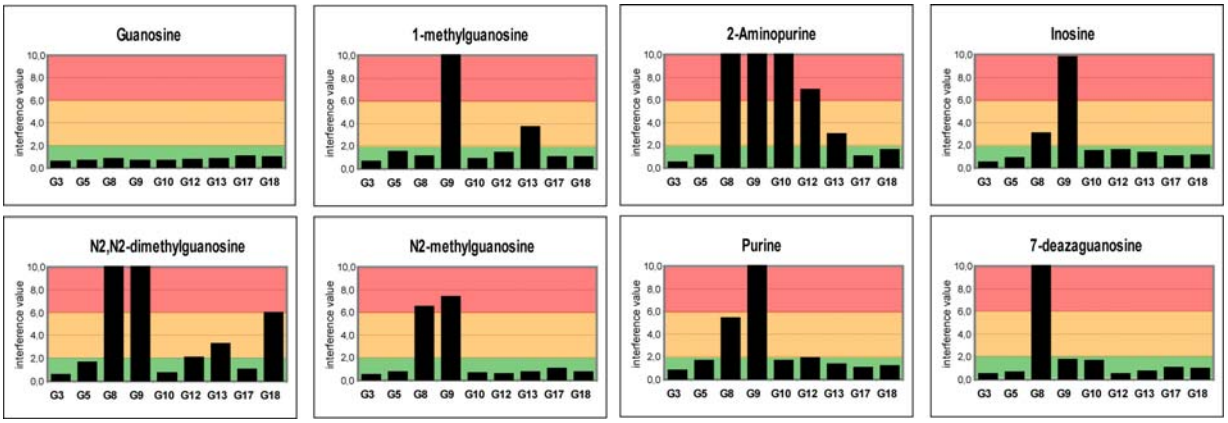

Figure S5. Interference values for 7S11 dNAIM libraries.

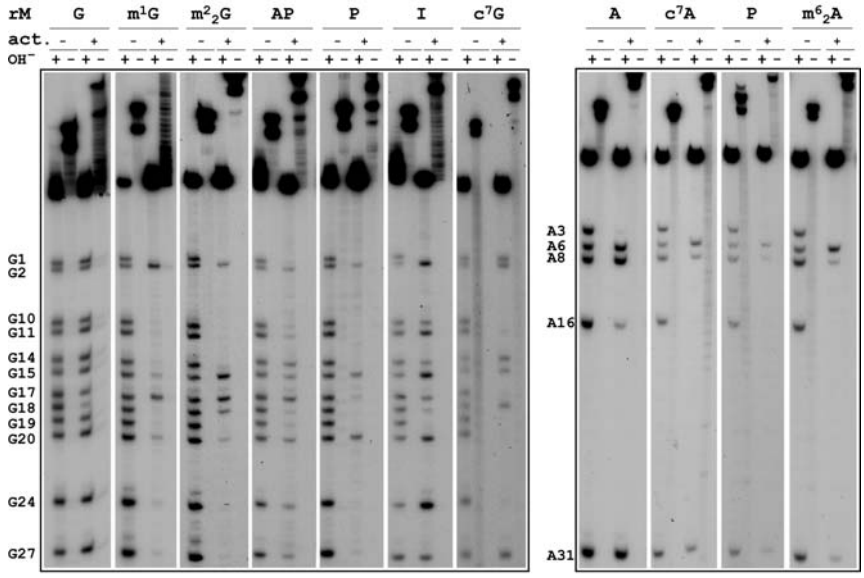

Figure S6. Full images of alkaline hydrolysis gels of 9DB1* dNAIM libraries with purine nucleotide analogs.

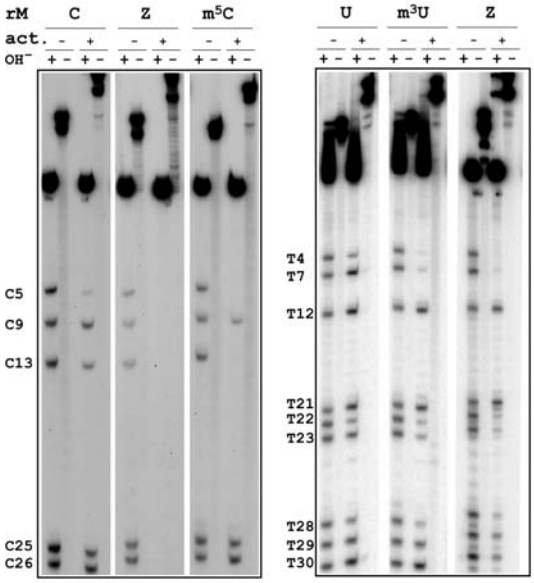

Figure S7. Full images of alkaline hydrolysis gels of 9DB1* dNAIM libraries with pyrimidine nucleotide analogs.

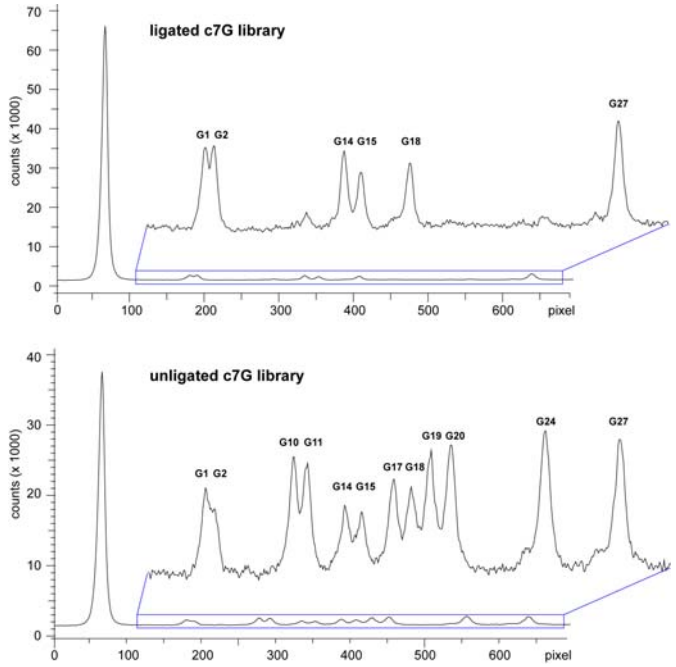

Figure S8. Example for line graph analysis of 9DB1* c^7G library. The integrated peak areas were used for calculation of the interference values.

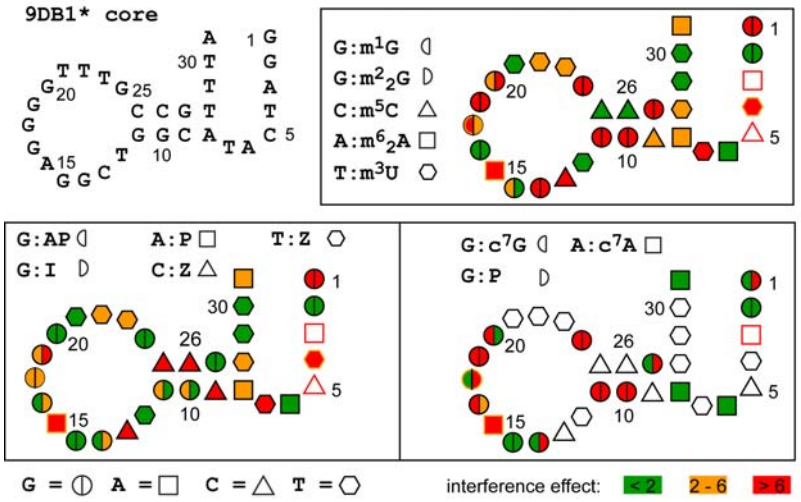

Figure S9. Schematic representation of interference effects in the 9DB1* catalytic core sequence for all nucleotide analogs used in dNAIM libraries. Colors represent strengths of interference effects (see also Figure 4 and S7). Nucleotide analogs grouped for introduction of steric effects (top) and functional group deletions at the Watson-Crick and Hoogsteen edges (bottom). Colored outline of nucleotide symbols indicate interference of the 2'-OH tag.

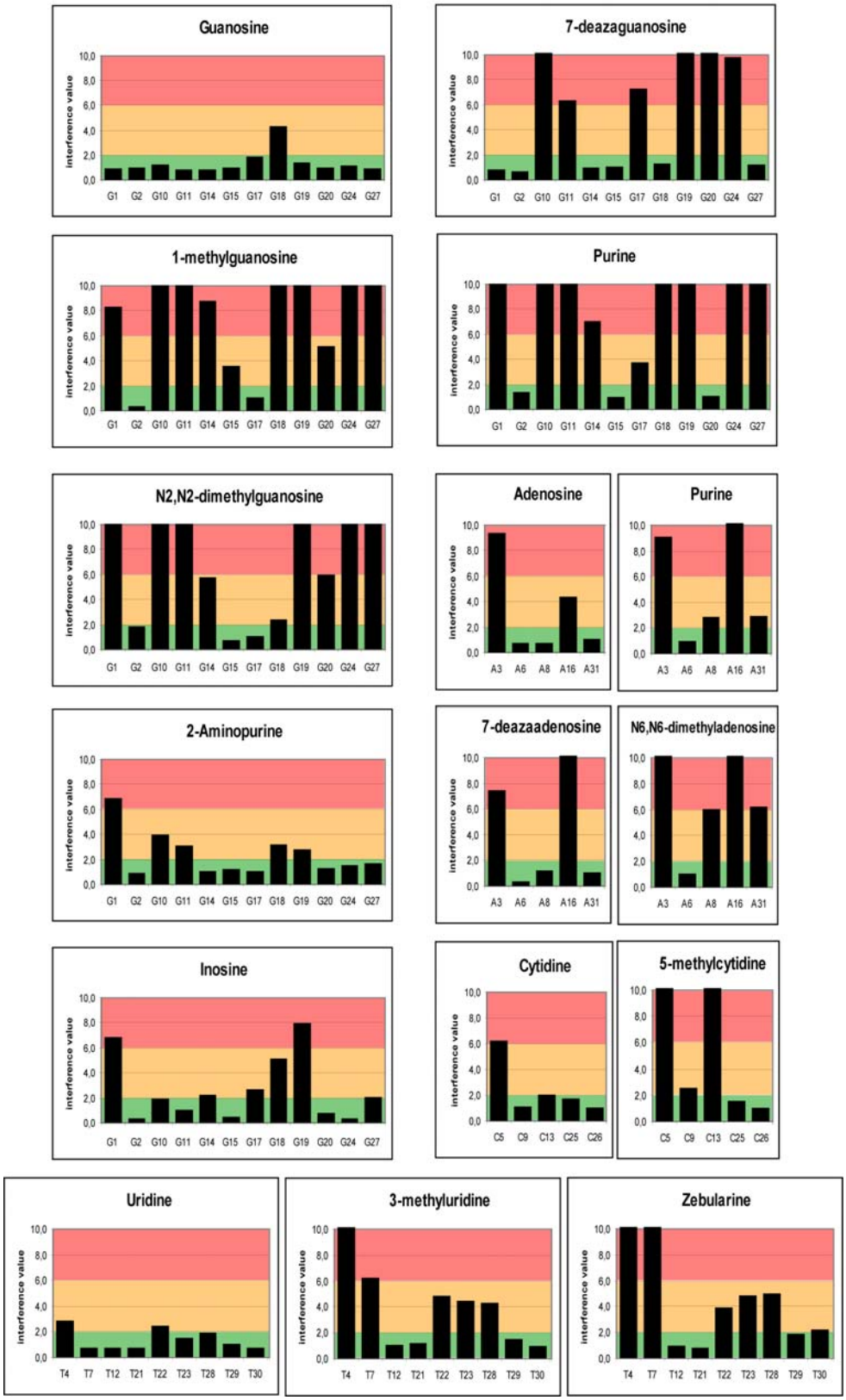

Figure S10. Interference values for 9DB1* dNAIM libraries.
(Interference values for Zebularine at C-positions were all >10; bar graph not shown)

References for Supporting Information

(1) Höbartner, C.; Kreutz, C.; Flecker, E.; Ottenschläger, E.; Pils, W.; Grubmayr, K.; Micura, R. *Monatshefte für Chemie / Chemical Monthly* **2003**, *134*, 851.
(2) Höbartner, C. Dissertation (PhD Thesis), University of Innsbruck, Austria, **2004**.
(3) Milligan, J. F.; Groebe, D. R.; Witherell, G. W.; Uhlenbeck, O. C. *Nucleic Acids Res.* **1987**, *15*, 8783.
(4) Wachowius, F.; Javadi-Zarnaghi, F.; Höbartner, C. *Angew. Chem. Int. Ed.* **2010**, *49*, 8504.
(5) Cochrane, J. C.; Strobel, S. A. *Curr. Protoc. Nucleic Acid. Chem.* **2004**, Unit 6.9.
(6) Waldsich, C. *Nat. Protoc.* **2008**, *3*, 811.